Supplementary Information

A Bilayer Theranostic Hydrogel Integrating Visual pH Monitoring with Synergistic Diabetic Wound Healing Treatment

Zhenkang Diao[1], Taotian Zhang[1], Yilin Jiang[3], Jiawei Lu[1], Tianyuan Chen[3], Mengxing Zhang[1], Dezheng Hu[1], Haozhou Shu[1], Qin Lin[2], Shiqi Huang[1,*], Ling Zhang[1,3]

1 College of Polymer Science and Engineering, Sichuan University, Chengdu, 610065, China;

2 Key Laboratory of Drug-Targeting and Drug Delivery System of the Education Ministry, West China School of Pharmacy, Sichuan University, Chengdu, 610041, China;

3 Institute of Systems Epidemiology,West China School of Public Health and West China Fourth Hospital, Sichuan University, Chengdu 61004l, China.

* Corresponding author.

Supplementary Methods

S1. Synthesis and Characterization of GelMA

Gelatin was dissolved in deionized water under continuous stirring at 50 ℃ to obtain a homogeneous solution. Methacrylic anhydride was subsequently added dropwise at a controlled rate of 0.2 mL min^{-1}, and the reaction was allowed to proceed for 2 h. The methacrylation process was terminated by the addition of PBS.[1]

^{1}H NMR spectra of gelatin and GelMA were recorded in D_2O to evaluate the degree of methacrylation (DM%). DM% was calculated according to Equation (S1):[2]

$$DM\% = 1 - \frac{peak\ area\ of\ GelMA\ lysine\ methylen}{peak\ area\ of\ gelatin\ lysine\ methylen} \times 100\#(S1)$$

FTIR spectroscopy was performed in the range of 4000–400 cm^{-1} to identify characteristic functional groups associated with methacrylation. XPS analysis was further conducted to examine surface elemental composition and chemical bonding states, including survey scans and high-resolution C 1s and O 1s spectra.

S2. Synthesis and Characterization of QLs

S2.1 Synthesis of QLs

QLs were fabricated via the thin-film hydration technique. Briefly, lecithin, cholesterol, PEG2000, and quercetin were mixed at a mass ratio of 13:4:1:6 and dissolved in a chloroform/methanol mixture. The organic solvent was removed by rotary evaporation to form a uniform lipid film,

which was subsequently hydrated with PBS. The resulting dispersion was probe-sonicated, filtered through a 0.45 μm membrane, and stored at 4 ℃ for further use [3]. Blank liposomes (BLs) were prepared following the same procedure without the addition of quercetin.

S2.2 Particle size and zeta potential analysis

The hydrodynamic diameter and size distribution of QLs were measured by dynamic light scattering (DLS), while the surface zeta potential was determined using electrophoretic light scattering at room temperature. All measurements were performed in triplicate.

S2.3 Morphological characterization

The morphology and structural features of the liposomes were primarily examined by transmission electron microscopy (TEM). Fresh liposome suspensions were deposited onto carbon-coated copper grids, negatively stained with phosphotungstic acid, and dried at room temperature prior to observation. TEM images enabled direct visualization of vesicle size, spherical morphology, and lamellar structure.

Scanning electron microscopy (SEM) was additionally employed to evaluate the surface morphology of freeze-dried liposomes. Samples were freeze-dried, mounted on conductive adhesive tape, sputter-coated with a thin gold layer, and imaged at an appropriate accelerating voltage.

S2.4 Encapsulation efficiency and drug loading

The encapsulation efficiency (EE%) and drug loading capacity (DL%) of QLs were determined by quantifying unencapsulated quercetin. Free quercetin was separated from liposomes by centrifugation (12,000 rpm, 20 min, 4 ℃), and the supernatant was analyzed using high-performance liquid chromatography (HPLC).

HPLC analysis was conducted using an acetonitrile/0.1% phosphoric acid aqueous solution (30:70, v/v) as the mobile phase, with a detection wavelength of 360 nm, column temperature of 30 ℃, flow rate of 1.0 mL min^{-1}, and injection volume of 10 μL. The amount of encapsulated quercetin was calculated by subtracting the free drug content from the total amount added. EE% and DL% were calculated using Equations (S2) and (S3):

$$\%EE = \frac{c_t - c_f}{c_t} \times 100\#(S2)$$

$$\%DL = \frac{W_{encapsulated}}{W_{lipdis}} \times 100\#（S3）$$

where $c_t$represents the total quercetin concentration, $c_f$denotes the concentration of free quercetin in the aqueous phase, and W_{lipids}refers to the total mass of lipids used for liposome preparation.

S2.5 In vitro release of quercetin from G–GS@QC

The in vitro release behavior of quercetin from G–GS@QC hydrogels was evaluated by immersing a predetermined amount of hydrogel in 50 mL of PBS containing 0.5% (w/v) Tween 80. The release study was carried out

at 37 ℃ under continuous shaking at 120 rpm. At predefined time points, 1 mL of release medium was withdrawn and replaced with an equal volume of fresh medium.

Collected samples were mixed with a tenfold volume of methanol, centrifuged, and the supernatant was analyzed by HPLC under the conditions described above. The cumulative release percentage was calculated according to Equation (S4)[4]

$$\text{Cumulative release (\%)} = \frac{VC_n + \sum_{i=1}^{n-1} V_s C_i}{W_0} \times 100\% \#(S4)$$

where $C_n$is the concentration of quercetin at the nth sampling point, $C_i$is the concentration at the ith sampling point, $V$is the total volume of release medium, $V_s$is the sampling volume, and W_0 is the initial amount of quercetin encapsulated in the liposomes.

2.6 Storage Stability of QLs

The storage stability of QLs was evaluated by monitoring changes in particle size and zeta potential. Liposomal dispersions were stored in sealed glass vials at 4 ℃ for up to 10 days. At predetermined time points, samples were withdrawn and analyzed to assess variations in particle size distribution and surface charge, thereby evaluating the colloidal stability of the liposomes during storage.

S3. Fabrication and detailed characterization of G–GS@QC hydrogels

S3.1 Design and fabrication of the bilayer hydrogel system

The lower layer of the bilayer hydrogel was composed of GelMA incorporated with SA, QLs, and Cu^{2+} ions, while the upper layer consisted of GelMA containing BTB as a pH-sensitive indicator. GelMA, photoinitiator, and other components were dissolved in deionized water at 35 °C to obtain homogeneous pre-gel solutions. For single-layer hydrogels, the pre-gel solution was exposed to ultraviolet (UV) irradiation at 365 nm for 90 s to induce photocrosslinking. The detailed formulations of the hydrogels are summarized in Table S1.

Table S1. Composition of Single-Layer and Bilayer Hydrogels

Hydrogel group	Layer	GelMA (w/v%)	SA (w/v%)	LAP (w/v%)	Quercetin liposomes（mg/g）	BTB	Cu^{2+}
G	Single	7.5	0	0.025	0	0.024	-
GS@QC	Single	7.5	1	0.025	100	-	-
G-GS@QC	Upper	7.5	0	0.025	0	0.024	-
	Lower	7.5	1	0.025	100	-	√

S3.2 Chemical structure and composition analysis

The chemical structure and composition of the hydrogels were analyzed by Fourier transform infrared spectroscopy (FTIR, 4000–400 cm^{-1}), X-ray diffraction (XRD, Cu Kα radiation, 2θ = 5–90°), and X-ray photoelectron spectroscopy (XPS). XPS survey spectra and high-resolution C 1s, O 1s, and Cu 1s spectra were collected using freeze-dried samples. Binding energies were referenced to the C 1s peak at 284.8 eV

and fitted accordingly.

S3.3 Microstructural characterization

The internal microstructure of the hydrogels was examined by SEM and cryogenic scanning electron microscopy (cryo-SEM). For SEM analysis, samples were frozen in liquid nitrogen, fractured, freeze-dried, sputter-coated with gold, and imaged. To preserve the native hydrated pore architecture, cryo-SEM was conducted by freezing and cryo-fracturing the samples, followed by controlled sublimation and imaging under cryogenic conditions, thereby minimizing dehydration-induced structural collapse.

S3.4 Mechanical and rheological properties

Compressive mechanical testing was performed using cylindrical hydrogel specimens (10 mm in diameter and 4 mm in thickness) on a universal testing machine at a crosshead speed of 10 mm min^{-1}. Reported values represent the mean of at least three independent measurements.

Rheological measurements were carried out using a parallel-plate rheometer (40 mm plate diameter). Disk-shaped samples (8 mm in diameter and 3 mm in thickness) were tested at 20 ℃. Strain sweep tests were conducted from 0.1% to 100% at a frequency of 1 Hz, followed by frequency sweep measurements from 0.1 to 100 Hz at a fixed strain of 1%.

The self-recovery behavior of the hydrogels was further evaluated by cyclic strain tests. Alternating strain cycles of 20% and 80% were applied,

with each strain level maintained for 60 s per cycle. The storage modulus (G′) and loss modulus (G″) were continuously recorded to assess the recovery capability of the hydrogel network after large deformation.

S3.5 Swelling behavior

The swelling behavior of the hydrogels was evaluated by immersing samples (1.0 g, n = 3) in 10 mL of PBS at 20 ℃. At predetermined time points, the samples were removed, gently blotted to remove surface liquid, and weighed until swelling equilibrium was reached. The swelling ratio (SR) was calculated according to Equation (S5):

$$\mathrm{SR} = \frac{W_t - W_0}{W_0} \times 100\% \#(S5)$$

Here, W_0 and W_t denote the dry weight and the swollen weight at time, respectively.

S4. Systematic investigations of biocompatibility, anti-inflammatory activity, and antioxidant capacity

S4.1 In vitro cytocompatibility

The in vitro cytocompatibility of G-GS, G-GS@Q, and G-GS@QC hydrogels was evaluated using a CCK-8 assay with L929 fibroblasts. Disk-shaped hydrogels (10 mm in diameter and 4 mm in thickness) were sterilized by UV irradiation and incubated in 10 mL of sterile DMEM at 37 ℃ with shaking at 100 rpm for 72 h to obtain hydrogel extracts. During extraction, daily UV exposure (2 h) was applied to minimize microbial

contamination. The extracts were centrifuged at 3000 rpm for 10 min and filtered through a 0.22 μm membrane to obtain 100% (v/v) extract solutions.

L929 cells in the logarithmic growth phase were seeded in 96-well plates at a density of 2 × 10^4 cells per well and cultured for 12 h prior to treatment. The medium was replaced with hydrogel extracts, and cells were incubated for 12, 24, and 36 h. At each time point, CCK-8 reagent was added, and absorbance at 450 nm was recorded. Cell viability was calculated using Equation (S6):

$$\text{Cell viability (\%)} = \frac{OD_{\text{sample}} - OD_{\text{blank}}}{OD_{\text{control}} - OD_{\text{blank}}} \times 100\% \#（S6）$$

S4.2 Hemocompatibility assessment

Hemocompatibility was evaluated using red blood cells (RBCs) isolated from Sprague–Dawley rats. RBCs were washed three times with PBS and diluted to a 2% (v/v) suspension. The RBC suspension was incubated with hydrogel samples at 37 ℃ for 2 h. PBS and deionized water were used as negative and positive controls, respectively. After centrifugation, the supernatants were collected for visual inspection and absorbance measurement at 540 nm. The hemolysis ratio was calculated according to standard protocols.

S4.3 In vitro anti-inflammatory evaluation

RAW 264.7 macrophages were cultured in high-glucose DMEM

supplemented with 10% FBS at 37 ℃ in a humidified atmosphere containing 5% CO_2. Cells were seeded at a density of 2×10^6 cells mL^{-1} and allowed to adhere for 12 h. An inflammatory model was established by treating cells with hydrogel-derived extracts supplemented with LPS (1000 ng mL^{-1}) for 12 h.[5]

After stimulation, culture supernatants were collected and centrifuged at 12,000 rpm for 10 min. The levels of pro-inflammatory cytokines, including IL-6, IL-1β, and TNF-α, were quantified using ELISA kits. For gene expression analysis, cells were lysed after PBS washing, and qPCR was performed using primers listed in Table S2.

Table S2. Primer sequences used for qRT-PCR

Gene	Forward primer (5′–3′)	Reverse primer (5′–3′)
IL6	TAGTCCTTCCTACCCCAATTTCC	TTGGTCCTTAGCCACTCCTTC
IL1b	GGGCTGCTTCCAAACCTTTG	AAGACACAGGTAGCTGCCACA
Nos2	CGGCAAACATGACTTCAGGC	GCACATCAAAGCGGCCATAG
Mrc1	ATGGATTGCCCTGAACAGCA	TGTACCGCACCCTCCATCTA
Gapdh	AGGTCGGTGTGAACGGATTTGA	TGTAGACCATGTAGTTGAGGTCA

S4.4 Intracellular ROS-scavenging evaluation

The antioxidant capacity of the hydrogels was assessed by measuring intracellular ROS levels in RAW 264.7 macrophages. After treatment with hydrogel samples, cells were exposed to H_2O_2 to induce oxidative stress. Intracellular ROS levels were detected using the fluorescent probe DCFH-DA following the manufacturer's instructions. Fluorescence intensity was

recorded, and ROS-scavenging efficiency was calculated by normalization to the control group.

S5. In vitro and in vivo antibacterial evaluation

S5.1 Agar plate antibacterial assay and colony counting analysis

The antibacterial activity of the G-GS@QC hydrogel against Staphylococcus aureus, MRSA, and Escherichia coli was evaluated using an agar plate spreading method. Bacterial suspensions in the logarithmic growth phase were diluted to approximately 1×10^7 CFU • mL^{-1} and spread onto LB agar plates. After treatment with PBS (Ctrl) or G-GS@QC hydrogel at 37 ℃, the bacterial suspensions were re-plated on fresh LB agar plates and incubated overnight. Colony-forming units (CFU) were counted and converted into $\log_{10}$ CFU·mL^{-1} values. All experiments were performed in triplicate, and antibacterial rates were calculated relative to the Ctrl group.

S5.2 Bacterial morphology observation

Bacterial morphology after different treatments was observed by SEM and TEM. For SEM analysis, bacteria were fixed with 2.5% glutaraldehyde, dehydrated with graded ethanol, dried, sputter-coated with gold, and imaged under SEM. For TEM analysis, bacterial suspensions were negatively stained with 2% phosphotungstic acid on copper grids and observed under TEM after natural drying.

S5.3 Live/dead bacterial staining

To further assess bacterial viability, a live/dead bacterial staining assay was performed using a DMAO/PI staining kit. After treatment with PBS (CTRL) or G-GS@QC hydrogel, bacterial suspensions were collected and incubated with DMAO and PI dyes according to the manufacturer's instructions at 37 ℃ in the dark for 15 min.

The stained bacteria were then observed using confocal laser scanning microscopy. In this assay, viable bacteria are labeled by DMAO, while bacteria with compromised membranes are stained by both DMAO and PI, appearing as merged signals. This method was used to qualitatively evaluate bacterial viability after different treatments.

S5.4 In vivo antibacterial evaluation

The in vivo antibacterial performance of the hydrogel was evaluated using a diabetic infected wound model in rats. To establish the diabetic model, animals were first fed a high-fat diet for 1 week, followed by intraperitoneal injection of streptozotocin (STZ) at a dose of 30 mg/kg for five consecutive days. [6] Prior to each injection, the rats were fasted for 12 h. Blood glucose levels were monitored, and rats with consistently elevated glucose levels were considered diabetic.

After successful induction of diabetes, full-thickness skin wounds were created on the dorsal region of the rats. A mixed bacterial suspension of *E. coli* and *S. aureus* (1×10^8 CFU·mL^{-1}, 1:1 ratio) was prepared, and

50 μL of the suspension was applied onto each wound to establish an infected wound model.

The animals were randomly divided into two groups: Ctrl and G-GS@QC. The Ctrl group received only sterile shoulder bandaging without any treatment, while the G-GS@QC group received hydrogel dressing applied directly to the wound surface. Dressings were replaced at predetermined time points, and wound healing was monitored throughout the experiment.

At designated time points (day 3 and 5), wound tissues were harvested, homogenized in PBS, serially diluted, and plated on agar plates for bacterial culture and colony counting. The inhibition rate was calculated according to the following formula:

$$Inhibition\ rate\ (\%) = \frac{N_{CTRL} - N_{sample}}{N_{CTRL}} \times 100\% \#(S8)$$

where N_{CTRL} and N_{sample} epresent the bacterial colony counts of the Ctrl and treatment groups, respectively.

Additionally, wound tissues were collected for histological analysis, including H&E staining, Masson's trichrome staining, and Gram staining, to assess inflammation, collagen deposition, and bacterial presence, respectively.

S6. In vivo evaluation of G-GS@QC hydrogel for diabetic chronic wound healing

S6.1 Establishment of a type II diabetic rat model

Forty male Sprague–Dawley rats (6–8 weeks old, ~200 g) were acclimatized for one week under standard conditions with free access to food and water. A type 2 diabetes mellitus rat model was established via high-fat diet feeding combined with 30 mg/kg STZ continuous injection. Rats with stable hyperglycemia were selected for subsequent wound healing experiments.

S6.2 Construction of a full-thickness diabetic skin wound model

Diabetic rats were anesthetized, and dorsal hair was removed followed by skin disinfection. Circular full-thickness excisional wounds with a diameter of 10 mm were created on the dorsal skin using a biopsy punch to establish a standardized wound model.

S6.3 In vivo wound healing evaluation

Animals were randomly divided into five groups (n = 5): healthy control (HC), diabetic control (DC), and diabetic rats treated with G-GS, G-GS@Q, or G-GS@QC hydrogels.

All hydrogels were sterilized by ultraviolet irradiation prior to use. Immediately after wound creation, the corresponding hydrogel was applied to fully cover the wound area. For HC and DC groups, an equal volume of

sterile saline was applied. Wounds were then covered with a transparent polyurethane dressing, and Elizabethan collars were fitted to prevent interference.

Dressings were replaced every two days for a total of three replacements. Digital photographs of wounds were taken on days 0, 3, 7, and 14. Residual wound areas were quantified using ImageJ software. The wound healing ratio was calculated as:

$$Healing\ ratio = \frac{A - A_T}{A} \times 100\% \#(S7)$$

where A represents the initial wound area and^{A_T} denotes the wound area at time T.

S6.4 Histological and systemic toxicity evaluation

At designated time points, rats were weighed, anesthetized, and euthanized. Peri-wound skin tissues and major organs (heart, liver, spleen, and lung) harvested on day 14 were fixed in 4% paraformaldehyde, embedded in paraffin, sectioned, and subjected to histological analysis.

Hematoxylin and eosin (H&E) staining was performed to assess tissue regeneration and potential systemic toxicity. In addition, inflammatory cytokines (TNF-α, IL-6, IL-10, and IL-1β) in wound homogenates were quantified using ELISA kits.

S6.5 Hematological, serum biochemical, and histological analysis

Following euthanasia, whole blood samples were collected. Part of

the samples was used for routine hematological analysis, including hematocrit (HCT), hemoglobin (HGB), lymphocyte count (LYM), mean corpuscular hemoglobin (MCH), mean corpuscular volume (MCV), plateletcrit (PCT), platelet count (PLT), red blood cell count (RBC), and white blood cell count (WBC). The remaining blood samples were centrifuged to obtain serum for biochemical analysis of C-reactive protein (CRP), lactate dehydrogenase (LDH), triglycerides (TG), and albumin (ALB), enabling a comprehensive evaluation of biosafety. In addition, major organs (heart, liver, spleen, lung, and kidney) were harvested, fixed, sectioned, and subjected to histological examination to assess potential organ toxicity.

Supplementary Figures

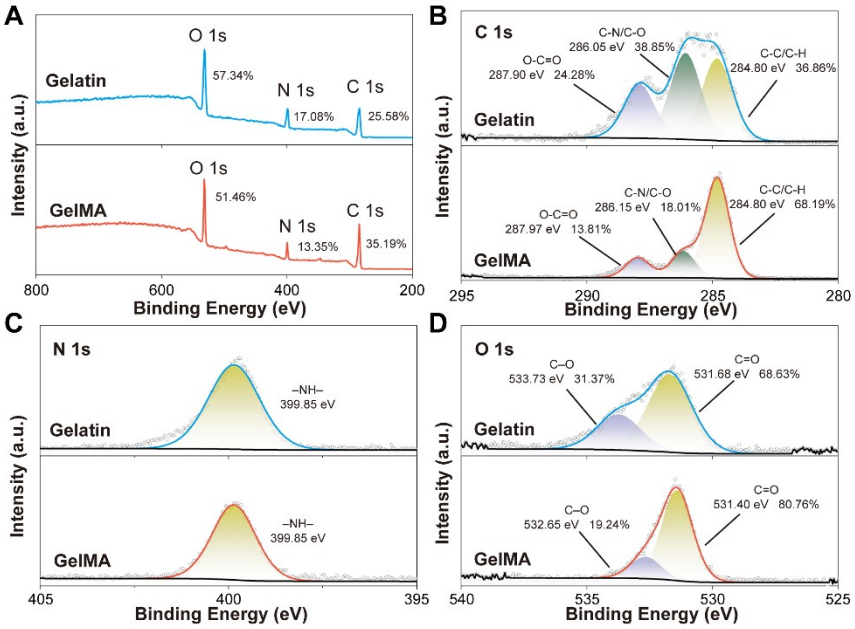

Figure S1. XPS analysis of gelatin and GelMA.

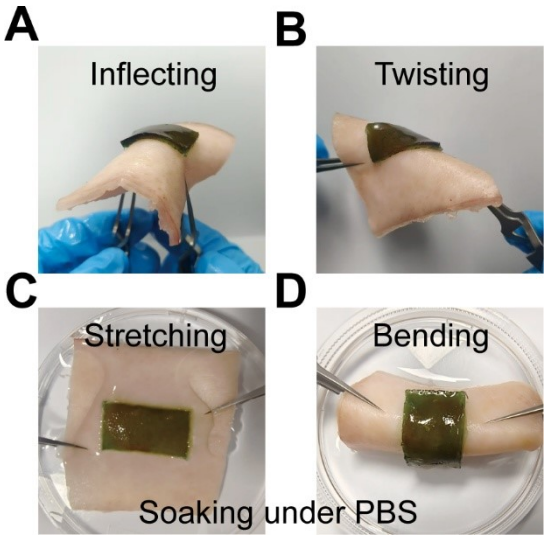

Figure S2. Adhesive performance of the G–GS@QC hydrogel on porcine skin using an ex vivo model that simulates the biological interface. (A, B) Adhesion under inflecting and twisting in dry conditions. (C, D) Adhesion after PBS immersion under stretching and bending, mimicking a moist wound environment.

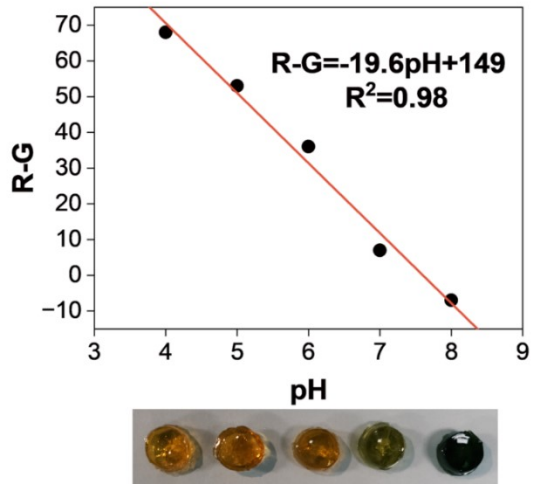

Figure S3. R-G ratio of the single-layer G hydrogel at different pH values, along with representative photographs illustrating the color changes of the single-layer G hydrogel over the pH range of 4–8.

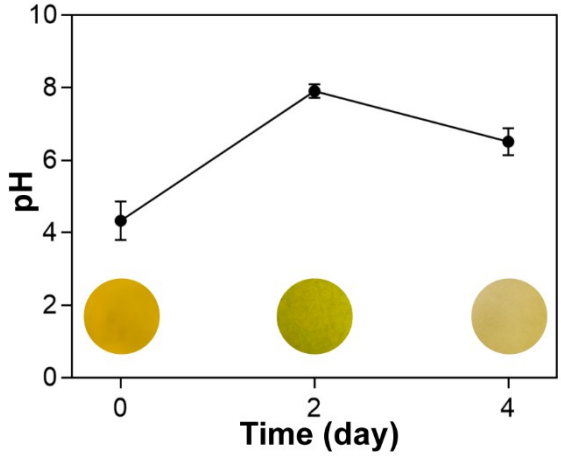

Figure S4. Photographs and pH variation of the G-GS@QC hydrogel at day 0, 2, and 4.

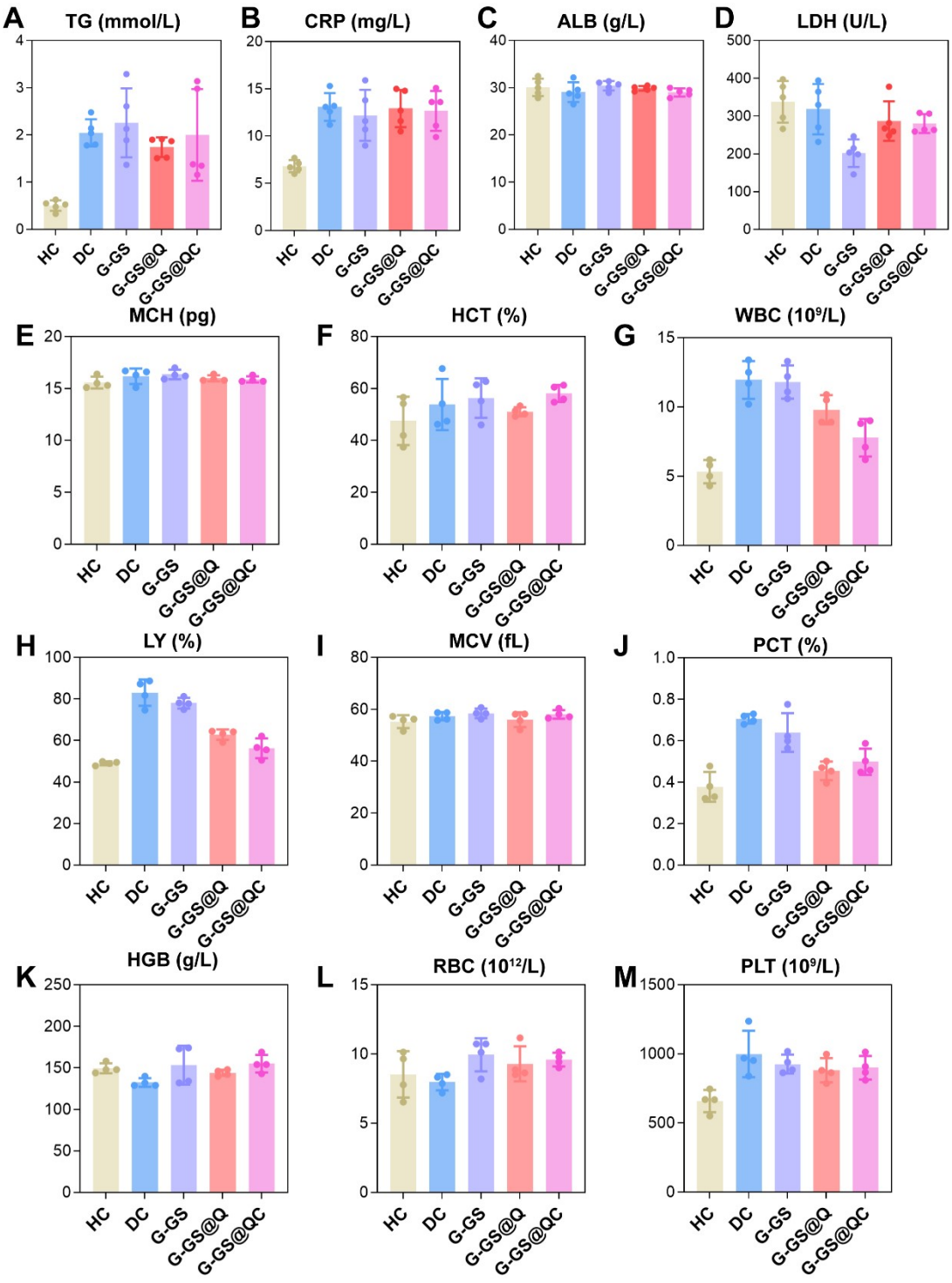

Figure S5. Hematological and serum biochemical analysis after different treatments.

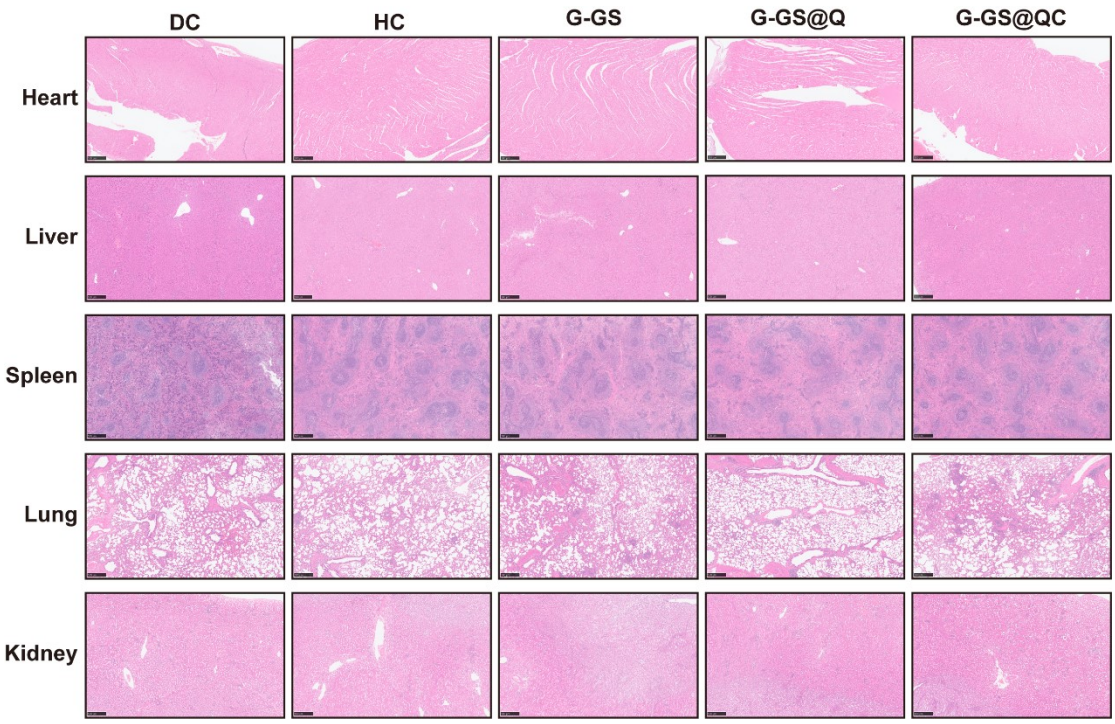

Figure S6. Histological evaluation of major organs after treatment. Representative H&E staining images of heart, liver, spleen, lung, and kidney harvested from different groups. Scale bar = 500 μm.

References

[1] K. Yue, G. Trujillo-de Santiago, M.M. Alvarez, A. Tamayol, N. Annabi, A. Khademhosseini, Synthesis, properties, and biomedical applications of gelatin methacryloyl (GelMA) hydrogels, Biomaterials 73 (2015) 254–271. https://doi.org/10.1016/j.biomaterials.2015.08.045.

[2] E. Hoch, C. Schuh, T. Hirth, G.E. Tovar, K. Borchers, Stiff gelatin hydrogels can be photo-chemically synthesized from low viscous gelatin solutions using molecularly functionalized gelatin with a high degree of methacrylation, J. Mater. Sci.: Mater. Med. 23 (2012) 2607–2617. https://doi.org/10.1007/s10856-012-4731-2.

[3] Z. Yuan, L. Chen, L. Fan, M. Tang, G. Yang, H. Yang, X. Du, G. Wang, W. Yao, Q. Zhao, B. Ye, R. Wang, P. Diao, W. Zhang, H. Wu, X. Zhao, Y.-Q. Wei, Liposomal Quercetin Efficiently Suppresses Growth of Solid Tumors in Murine Models, Clinical Cancer Research 12 (2006) 3193–3199. https://doi.org/10.1158/1078-0432.CCR-05-2365.

[4] S. Bohrey, V. Chourasiya, A. Pandey, Polymeric nanoparticles containing diazepam: preparation, optimization, characterization, in-vitro drug release and release kinetic study, Nano Convergence 3 (2016) 3. https://doi.org/10.1186/s40580-016-0061-2.

[5] B.M. Facchin, G.O. Dos Reis, G.N. Vieira, E.T.B. Mohr, J.S. da Rosa, I.F. Kretzer, I.G. Demarchi, E.M. Dalmarco, Inflammatory biomarkers on an LPS-induced RAW 264.7 cell model: a systematic review and meta-analysis, Inflamm. Res. 71 (2022) 741–758. https://doi.org/10.1007/s00011-022-01584-0.

[6] M. Zhang, X.-Y. Lv, J. Li, Z.-G. Xu, L. Chen, The characterization of high-fat diet and multiple low-dose streptozotocin induced type 2 diabetes rat model, J. Diabetes Res. 2008 (2008) 704045. https://doi.org/10.1155/2008/704045.